Visually-based color space tetrahedrizations for printing with custom inks

Sylvain M. Chosson, Roger D. Hersch

sylvain.chosson@epfl.ch, rd.hersch@epfl.ch
Ecole Polytechnique Fédérale de Lausanne (EPFL),
DI-LSP CH-1015 Lausanne, Switzerland.

ABSTRACT

Printing with custom inks is useful for extending the gamut of printed images, for creating artistically appealing designs or for providing protection against counterfeiting (security documents). The basic colors we consider, consist of the custom inks, their superpositions and the white paper. Color separation for custom inks requires to determine the relative amounts of the basic colors allowing to render each desired input color. To achieve this goal, one may tetrahedrize the set of basic colors on a given 3D color space. However, even for a few basic colors, there are many different tetrahedrizations (for example with 8 points in 3D space, one may build more than 120 different tetrahedrizations).

When printed at a very high resolution, i.e. when screen dots are not visible, different tetrahedrizations yield halftoned color images which look similar. However, in the case of large screen tiles or for sophisticated screens, the dither patterns may remain visible. When the halftone patterns are visible, certain tetrahedrizations yield well-behaved regular halftone patterns whereas other tetrahedrizations tend to create false contours due to successions of high and low frequency halftone patterns. We show that the standard Delaunay tetrahedrization yields visually poor results: transitions between tetrahedra with vertices having high luminance differences (CIE-LAB ΔL) and tetrahedra with vertices having low luminance differences yield false contours.

In the present paper, we experiment with various criteria for choosing the tetrahedrization yielding the least amounts of visual artifacts (false contours). Such criteria comprise the selection of tetrahedrizations which either (1) maximize the mean CIE-LAB ΔL value within the tetrahedra; (2) maximize the variance in ΔL ($Var_{\Delta L}$) within the tetrahedra; (3) constrain a maximum number of tetrahedra to have as a common edge the line connecting the darkest with the brightest basic color; or (4) constrain a maximum number of tetrahedra to have as one common vertex the darkest basic color. The results are illustrated with color wedges[a] crossing the printing gamut of the given custom inks.

Keywords: Custom inks, color separation, tetrahedrization, dithering, halftoning artifacts.

1. INTRODUCTION

Existing approaches for color separation with non-standard inks include: the creation of correspondence tables between input colors and combination of the output inks [1]; the selection of a subset of the output inks according to an objective function [2]; or the partition of the CIE-XYZ color space into a set of tetrahedra having as a common edge the black-white axis

a. Color wedges and dithered images are visible in the PDF version of this article located at URL *http://diwww.epfl.ch/w3lsp/publications/colour/* .
They are reproduced in the Appendix on the last page. Since no colorimetric calibration has been carried out, differently separated printed dithered images may be distant in terms of the reproduced colors.

Proceedings of SPIE, Jan. 2001, San Jose, USA
Color Imaging: Device-Independent Color, Color Hardcopy, and Graphic Arts VI
Vol. 4300, pages 81-92

[3,4]. We are interested in comparing various 3D color space tetrahedrizations for the color separation with a given set of custom inks.

A 3D color space can be segmented into several tetrahedra which ensure that each color of the printing gamut obtained by N custom inks can be printed as a combination of four basic printable colors. These four basic colors correspond to the vertices of the tetrahedron which surrounds the desired color in 3D color space. In order to synthesize the desired target color, multi-color dithering [5] converts relative color intensities into appropriate areas of basic colors. Different tetrahedrizations yield different dither patterns.

Dither patterns may be visible when looking at a printing image. Dither patterns are visible either due to screen elements which are too large in relation to the observation distance, or due to a low printing resolution. The appearance of dither pattern structure changes may be accentuated by an inadequate color separation.

The experiments we made with different tetrahedrizations lead to the conclusion that the tetahedrization of a color space must take into account printing inks properties such as their luminance. Artifacts due to an inappropriate tetrahedrization are discussed in section 4.

Several criteria are proposed in section 5 for the creation of tetrahedrizations minimizing dithering artifacts. We restrict the present study to the case of N=3 custom inks, their four possible superpositions and the paper's white.

2. TETRAHEDRAL SEPARATION

Let us consider three transparent custom colors C_1, C_2 and C_3, the 4 colors resulting from their superpositions C_1C_2, C_1C_3, C_2C_3 and $C_1C_2C_3$ and the paper's white C_w (Fig. 1). Their measured CIE-XYZ coordinates yield 8 points in the 3D color space.

Tetrahedrization methods and their properties are described in the literature [6]. A 3D color space volume specified by a set of basic colors can be subdivided into a set of adjacent mutually disjoint tetrahedra, whose vertices are the basic colors. Each point of the color gamut is contained within only one tetrahedron or at the common boundary of two or more tetrahedra. Input image colors which need to be rendered with the chosen set of basic colors are assumed to be located within the gamut formed by the printable colors. The problem of gamut mapping [7] is therefore out of the scope of the present article.

Each printable color can be reproduced by printing side by side an appropriate surfaces of four basic colors, selected from the inks and their superpositions. These four colors are the vertices of the tetrahedron which surrounds the desired color in the 3D color space. The amount of these 4 basic colors is obtained by a linear combination in the 3D color space, e.g. the barycentric interpolation weights of the tetrahedron's vertices [8].

With 3 inks and the resulting set of 8 basic colors, 70 different tetrahedra can be constructed (binomial coefficient C_4^8). More than 120 tetrahedrizations may be realized with 5 to more than 12 tetrahedra. Quality criteria should help us to reduce drastically the number of acceptable tetrahedrizations.

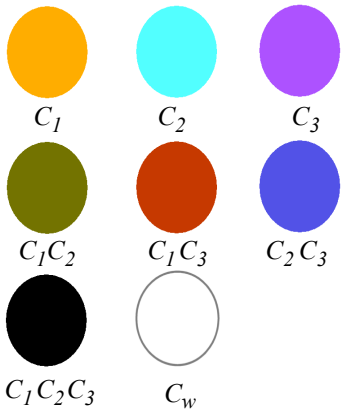

Figure 1. Set of basic colors.

3. MULTI-COLOR DITHERING

Multi-color dithering is an extension of standard bi-level dithering and is applied to convert relative amounts of basic colors to corresponding color surface coverages. As standard bi-level dithering, multi-color dithering requires the creation of a dither matrix. The dither threshold values of the dither matrix shown in Fig. 2a are placed so as to ensure that dots of the same color are clustered as much as possible in order to limit dot gain. These dither threshold values follow a space filling curve [9,10] as shown in Fig. 2b. Let us briefly review the basic principle of multi-color dithering [5].

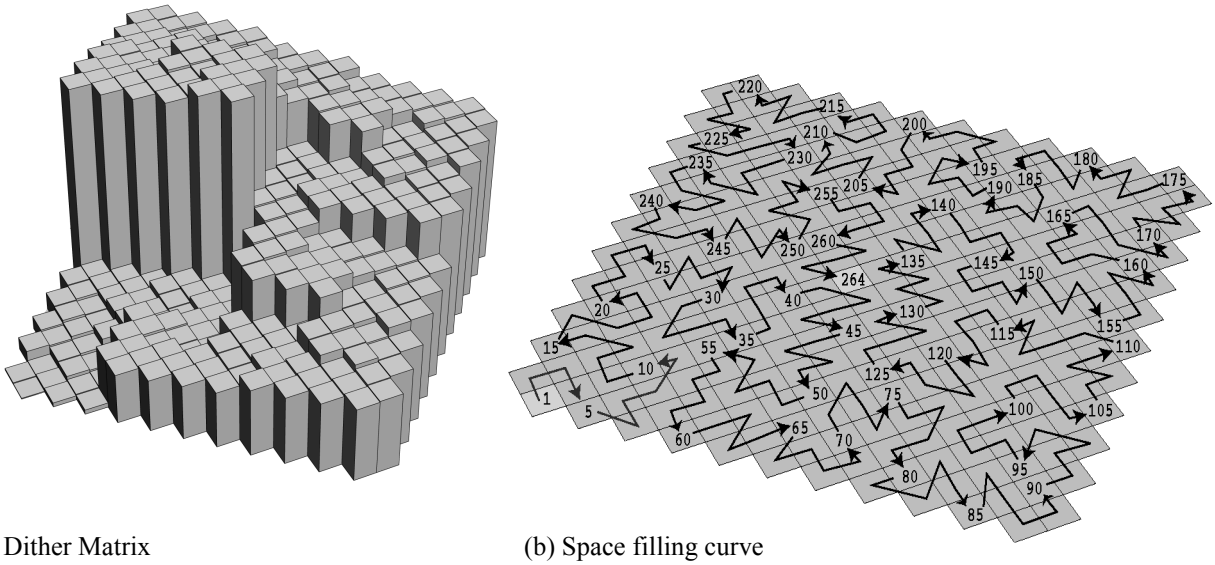

(a) Dither Matrix (b) Space filling curve

Figure 2. Space filling curve based dither matrix.

Consider an input image pixel of color C_i whose color coordinates in an output CIE-XYZ are located in a tetrahedron with vertices corresponding to the four basic colors C_1, C_2, C_3 and C_4. At each pixel of the output pixmap, the relative percentage of each of these basic colors is computed as a barycentric combination of C_1, C_2, C_3 and C_4, for example d_1 of color C_1, d_2 of color C_2, d_3 of color C_3 and d_4 of color C_4. Color C_i can be represented at the output image as an additive combination of these 4 amounts of color C_1, C_2, C_3 and C_4, placed side by side. Multi-color dithering allows to obtain the respective areas of each of the 4 colors which, when printed side by side, give the impression of color C_i.

An output image pixel is rendered with a color chosen among the 4 basic colors C_1, C_2, C_3 and C_4 as follows. To each output pixel at position {x,y} corresponds a threshold value Th(x,y) which is determined by the dither matrix. When the 4 relative amounts of basic colors $d_1(x,y)$, $d_2(x,y)$, $d_3(x,y)$ and $d_4(x,y)$ are evaluated, and assuming that the 4 colors C_1, C_2, C_3 and C_4 are ordered for instance according to their luminance value, the color chosen to represent pixel {x,y} in the output image (Fig. 3b), is color C_1 if $Th(x,y) \le d_1(x,y)$, C_2 if $d_1(x,y) < Th(x,y) \le d_1(x,y) + d_2(x,y)$, C_3 if $d_1(x,y) + d_2(x,y) < Th(x,y) \le d_1(x,y) + d_2(x,y) + d_3(x,y)$ and C_4 if $d_1(x,y) + d_2(x,y) + d_3(x,y) < Th(x,y)$.

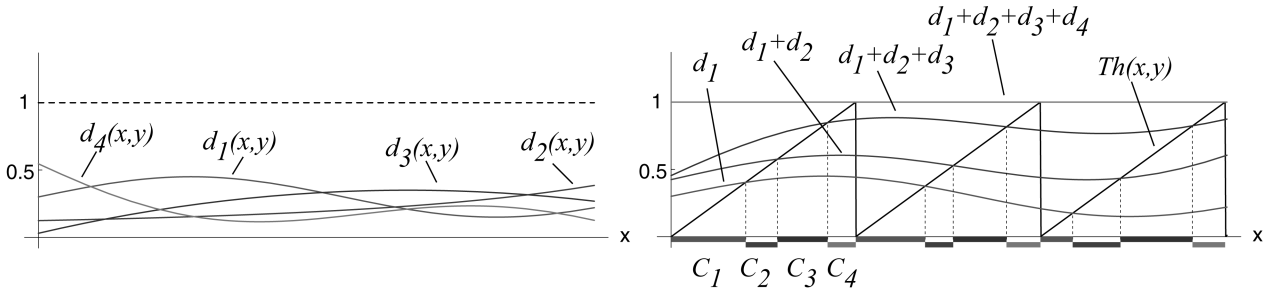

(a) Relative color intensities of 4 basic colors (b) Multi-color dithering

Figure 3. The principle of multi-color dithering.

4. DESCRIPTION OF THE ARTIFACT PHENOMENON

In the following analysis of color separation by tetrahedrization in 3D CIE-XYZ color space, point 1 stands for color C_1, point 2 for color C_2, point 3 for color C_3, point 4 for color C_1C_2, point 5 for color C_1C_3, point 6 for color C_2C_3, point 7 for color $C_1C_2C_3$ and point 8 for the paper's white (C_w).

The most widely used tetrahedrization of a set of points in 3D space is the Delaunay tetrahedrization. It has the property that the enclosing sphere of a tetrahedron does not include another point of the given point set. Delaunay tetrahedrization depends only on the coordinates of the considered points. Fig. 5a shows a color wedge whose vertices are located (Fig. 4 right) in the middle of the gamut edges 1-5, 4-7, 2-6 and 3-8. The wedge (Fig. 5a) is rendered with the color separation resulting from the Delaunay tetrahedrization of the 3D color space. Figure 4 left represents that wedge together with the intersecting tetrahedra.

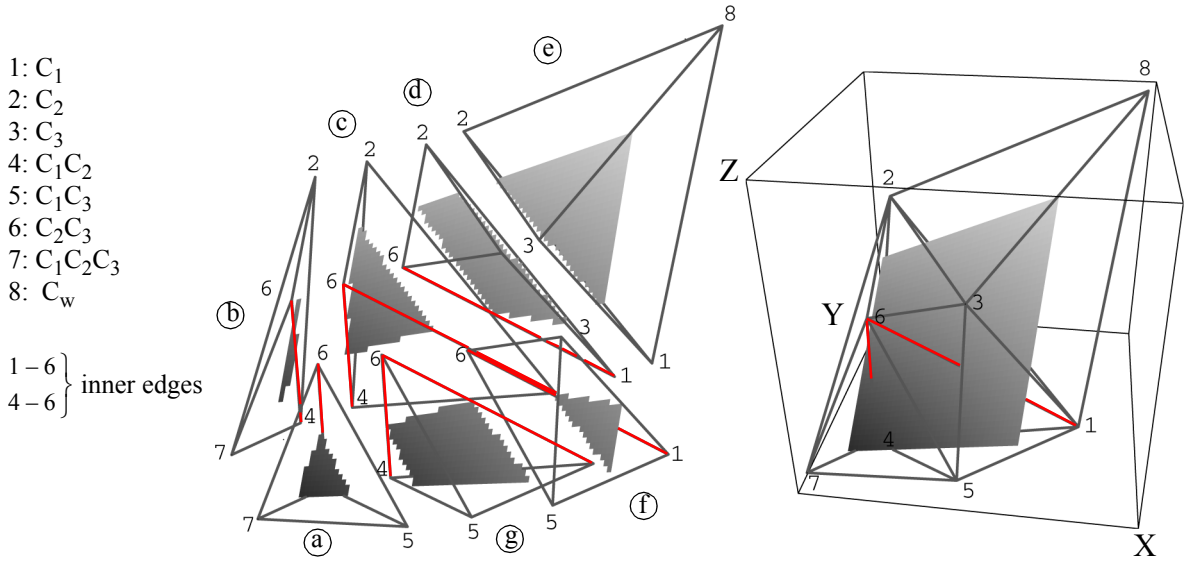

Figure 4. Delaunay tetrahedrization in an output XYZ space.

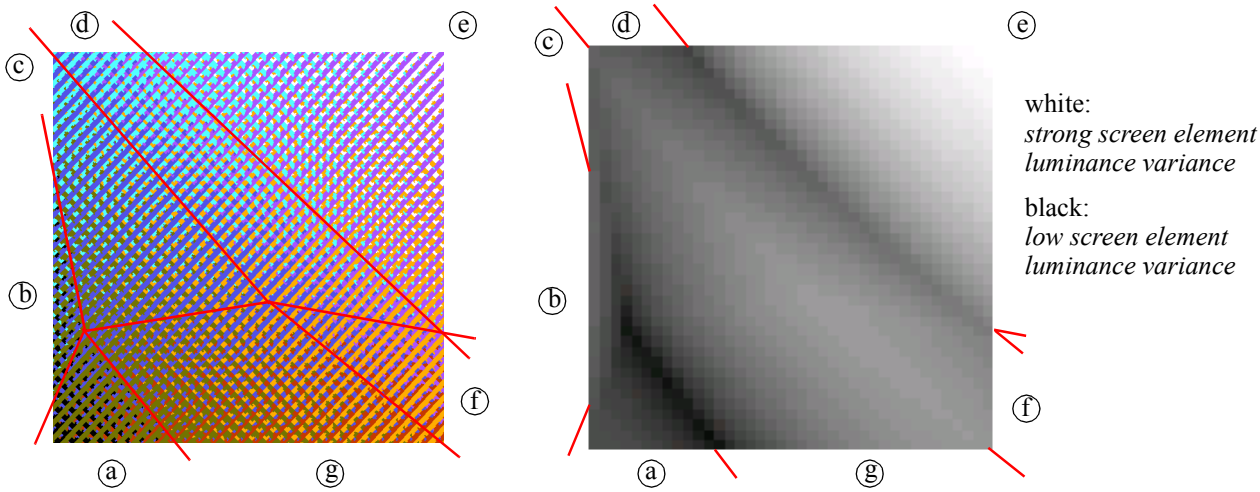

(a) Wedge (b) Screen element luminance variance

Figure 5. Color wedge produced with the Delaunay tetrahedrization.

At the bottom left of Fig. 5a, an artifact appears around the edge 4-6 (Fig. 4) and when the wedge crosses triangle 4-5-6. At the intersection of the wedge and the inner axis 4-6, the target color is produced by only two colors printed side by side (4 and 6). Through the tetrahedron face 4-5-6 the wedge incorporates a line printed with at most the 3 colors 4, 5 and 6. The artifact produced at the face 4-5-6 is due to the fact that the CIE-LAB L* luminances of colors 4, 5 and 6 are nearly equal,

whereas the wedge inside tetrahedron ⓐ (4-5-6-7) incorporates color 7 ($C_1C_2C_3$) having a very low luminance. Inside that tetrahedron, the wedge incorporates screen elements with strong luminance variations yielding a visible strong screen element frequency[a]. On the face 4-5-6 and inside tetrahedron ⓖ (1-4-5-6), screen elements do not incorporate luminance variations. This abrupt variation in visible screen element frequency produces the artifact. To a smaller extent, another artifact can be observed when passing from tetrahedron ⓓ (1-2-3-6) to tetrahedron ⓔ (1-2-3-8).

In order to quantify the variance in luminance responsible for the impact of the screen element frequency, let us define the screen element luminance variance (Var_L) where d_i represents the area covered by color C_i and L_i is the CIE-LAB luminance of color C_i.

$$Var_L = \frac{\sum_{i=1}^{4} (L_i - \bar{L})^2 \cdot d_i}{\sum_{i=1}^{4} d_i} \quad \text{where} \quad \bar{L} = \frac{\sum_{i=1}^{4} L_i \cdot d_i}{\sum_{i=1}^{4} d_i}$$

Fig. 5b shows a map of the luminance variance, where the lower the variance, the darker its representation. A low luminance variance represents a low amplitude of the screen element frequency.

Another possible tetrahedrization criterion consists in choosing the tetrahedrization yielding the greatest volume for each tetrahedron. Again, due to abrupt changes in luminance variance, there is a break in visible screen element frequency. "Greatest volume" tetrahedrization may lead to a tetrahedrization with only 5 tetrahedra. This is the lowest number of tetrahedra that can be obtained for a color separation with 8 basic colors (3 custom color inks, their 4 possible superpositions and white). This tetrahedrization does not incorporate a main axis, but it incorporates 4 inner faces (Fig. 6). To provide a halftone without false contours, i. e. without abrupt screen frequency amplitude variations, the luminance of each of the face's color vertices should differ from each other as much as possible.

Fig. 7a shows a color wedge passing through the 4 inner faces. There is a variation of the amplitude of the screen element frequency when traversing face 1-2-3 (ⓓ-ⓔ) as shown in Fig. 7b, but the slope is smooth enough to yield an acceptable dither image. The crossing of faces 1-3-7 (ⓐ-ⓔ), 1-2-7 (ⓑ-ⓔ) and 2-3-7 (ⓒ-ⓔ) is hardly detectable. These three faces comprise each vertices with three distant colors in terms of luminance, whereas colors 1, 2 and 3 have a similar luminance.

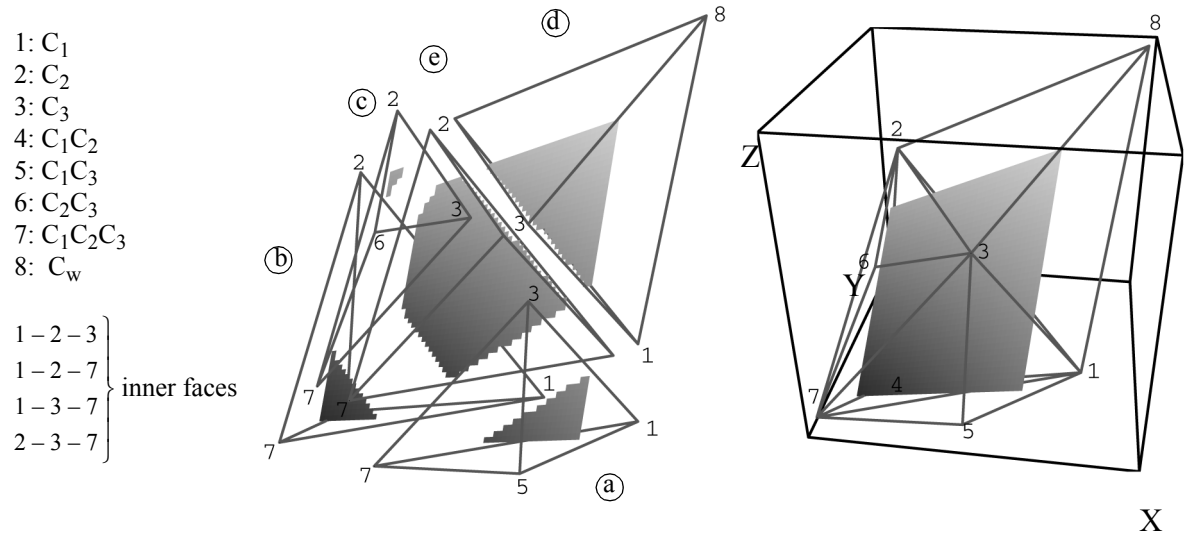

Figure 6. Tetrahedrization with 5 tetrahedra.

a. We define the *screen element frequency* by the two period vectors specifying the replication of the screen element within the dithered image. The screen element frequency is more or less visible according to its amplitude within specific regions of the image.

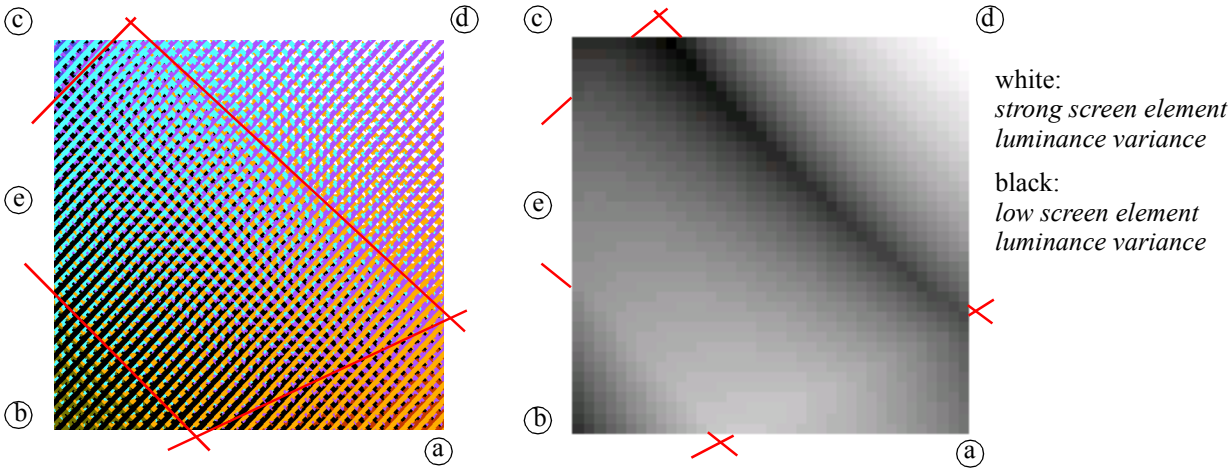

(a) Wedge (b) Screen element luminance variance

Figure 7. Color wedge produced with a tetrahedrization with 5 tetrahedra.

5. CRITERIA FOR THE CHOICE OF TETRAHEDRIZATIONS

As we have seen in the previous section, different tetrahedrizations of the given set of basic colors yield different dithered images. In order to avoid abrupt frequency variations when crossing the boundaries of tetrahedra, let us establish criteria for constructing tetrahedrizations minimizing the appearance of false contours. In the present contribution, tetrahedrizations are proposed and analyzed independently of the color content of the input image.

5.1. Maximizing mean luminance differences of tetrahedron's vertices

In one possible approach, the tetrahedra which make up the tetrahedrization should have the largest mean for their difference in luminance. This leads to tetrahedrizations with a high screen element frequency amplitude impact providing good visual results. The *mean tetrahedral luminance difference* is given by:

$$\overline{\Delta L_{N_t}} = \frac{1}{N_t} \sum_{T=1}^{N_t} \overline{\Delta L[T]} \quad \text{where} \quad \overline{\Delta L[T]} = \frac{1}{6} \sum_{i=1}^{3} \sum_{j=i+1}^{4} |L[T(i)] - L[T(j)]|$$

This formula computes the mean ($\overline{\Delta L_{N_t}}$), for the total number of tetrahedra (N_t), of the mean absolute differences ($\Delta L[T]$) between the luminances of each couple (6 couples) among the 4 vertices ($T(i)_{i=1,2,3,4}$) of a tetrahedron T.

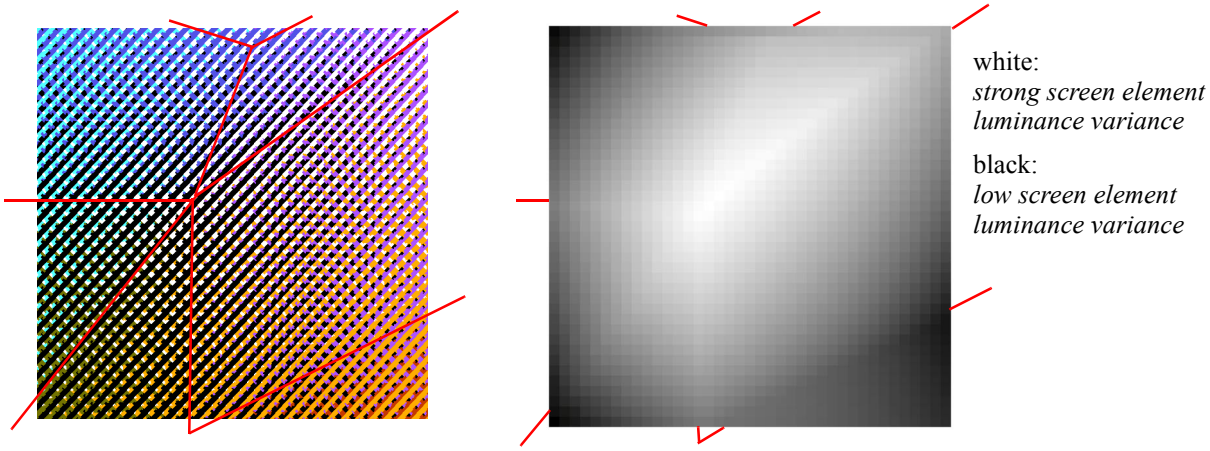

(a) Wedge (b) Screen element luminance variance

Figure 8. Color wedge produced with a tetrahedrization maximizing the mean luminance differences.

This criterion doesn't ensure that, when passing through the common face of two neighboring tetrahedra, no artifacts appear. It tends to produce tetrahedra which have vertices with sufficiently different luminances to keep the visible impact of the screen element frequency in most parts of the color gamut.

Figure 8 gives an example of a wedge rendered with the basic color set described in Fig. 1, for a tetrahedrization that maximizes the mean luminance differences. Figure 8b gives the screen element luminance variance for this wedge, which shows that the screen frequency amplitude is distributed very progressively across the wedge. At the corners of the wedge, the color components tend to be formed by couples of close colors, hence a decreasing screen frequency amplitude. At the top-right corner, the two colors 3 and 8 (Fig. 4) are distant in term of luminance and yield a strong screen element frequency amplitude.

In order to enforce a tetrahedrization along a strong luminance axis and to avoid tetrahedrizations with inner edges connecting vertices with similar luminance (for example Fig. 4, inner edge 4-6), let us introduce several proposals.

5.2. Maximizing the variance in luminance differences of tetrahedron's vertices

This criterion tends to create tetrahedra with long edges in the luminance direction and either maximize or minimize the luminance differences between tetrahedra vertices. It tends to avoid the appearance of short inner tetrahedron edges. Maximizing the variance of luminance differences doesn't ensure the removal of all short inner edges but ensures that all the tetrahedra have at least two easily distinguishable colors.

The following formula giving the variance in luminance differences produces the tetrahedrization with the most elongated tetrahedra along the dark-light orientation:

$$Var_{\Delta L} = \frac{1}{N_t} \sum_{a=1}^{N_t} \frac{1}{6} \sum_{i=1}^{3} \sum_{j=i+1}^{4} (|L[T_a(i)] - L[T_a(j)]| - \overline{\Delta L[T_a]})^2$$

For the chosen set of basic colors, the solution is identical to the one obtained by maximizing the mean luminance differences (Fig. 8). Further tetrahedrization solutions in decreasing order of $Var_{\Delta L}$ also yield nice results. For example, Fig. 9a shows the same wedge with the fifth tetrahedrization obtained with this criterion.

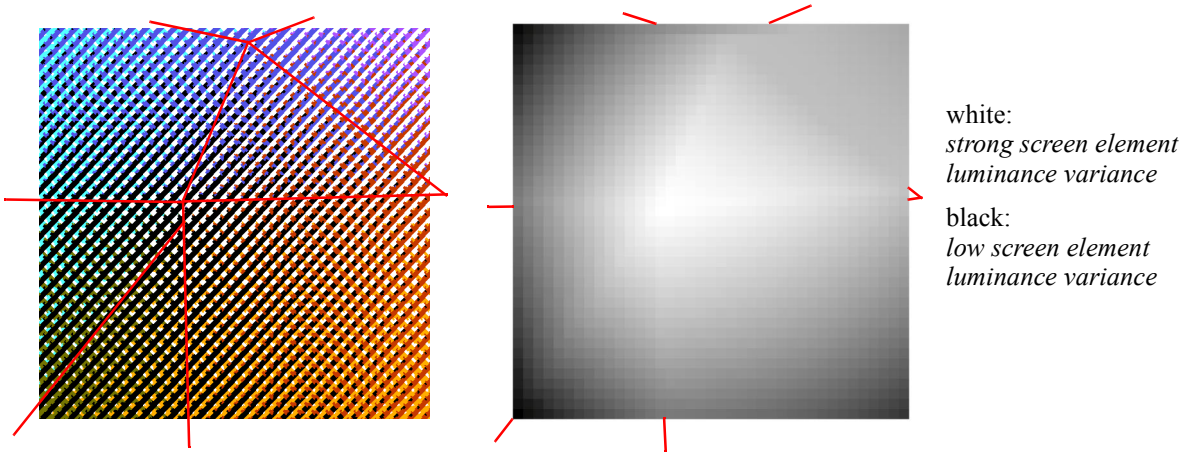

(a) Wedge (b) Screen element luminance variance

Figure 9. Color wedge produced with a tetrahedrization maximizing the variance in luminance differences.

5.3. Tetrahedrization with tetrahedra incorporating two vertices with the greatest luminance difference

Let us order the tetrahedrizations according to the number of tetrahedra having an edge between the 2 basic colors with the greatest luminance difference. The tetrahedrization with the highest ratio of tetrahedra having two vertices with the greatest luminance difference to the total number of tetrahedra is selected. We can also select the tetrahedrization where the ratio of the volume of these particular tetrahedra to the complete gamut volume is the largest. This last criterion ensures that the

majority of the gamut can be reproduced with always the same 2 colors printed side by side. The wedge of Fig. 11a shows that it can be produced without artifacts in terms of frequency breaks and without sudden changes of color components.

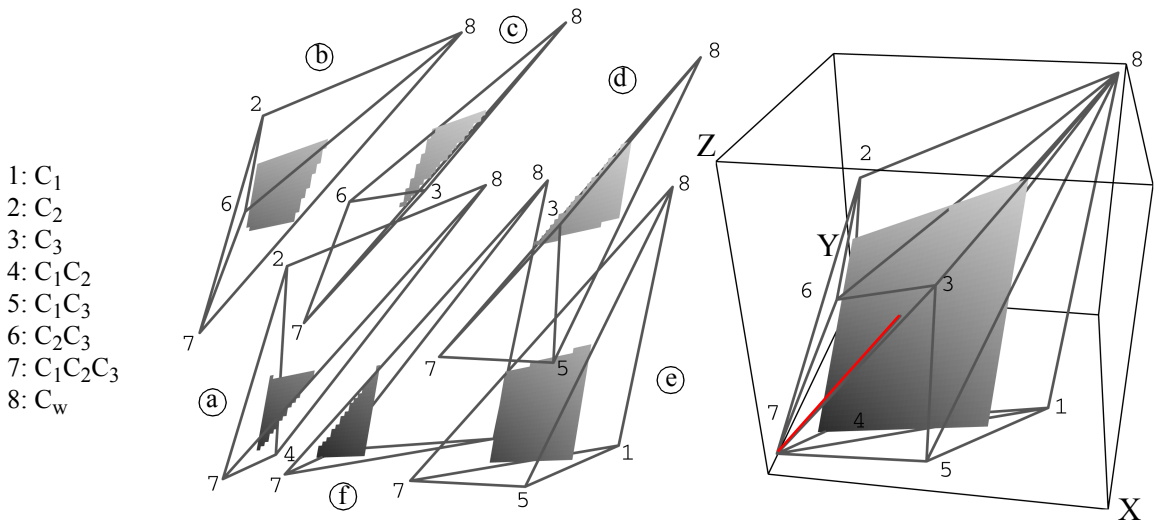

Figure 10. Tetrahedrization around the dark-white axis.

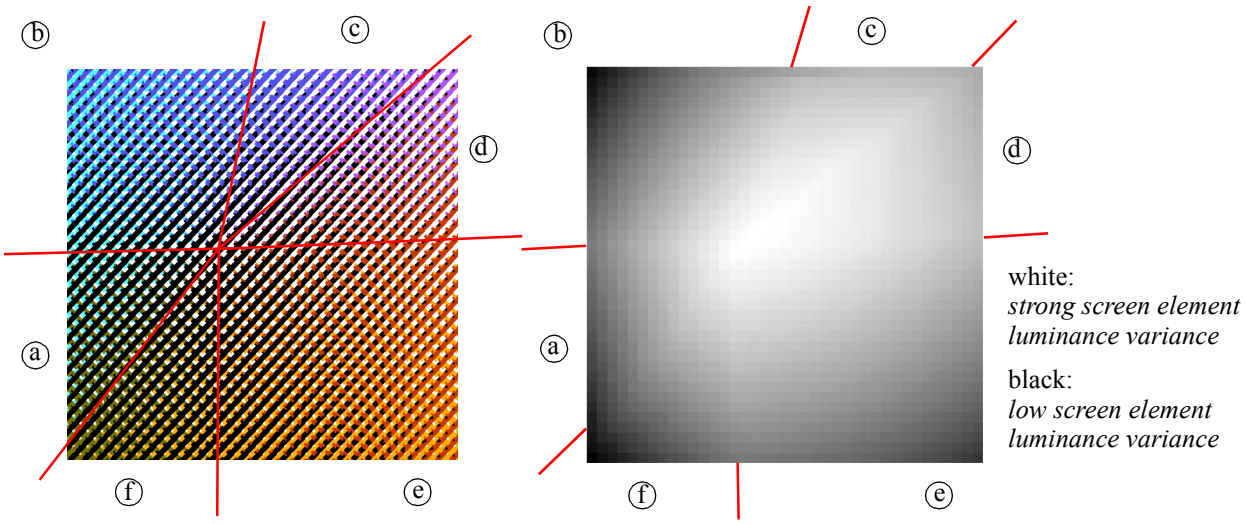

(a) Wedge (b) Screen element luminance variance

Figure 11. Color wedge produced with a tetrahedrization around the dark-white axis.

5.4. Tetrahedrization with a maximum of tetrahedra incorporating the darkest color

Let us select a tetrahedrization where a maximum number of tetrahedra incorporates the darkest color. Figure 12 shows the same wedge with the same basic colors but with the new tetrahedrization. With the variance representation shown in Fig. 13b, we can detect the place where there is a change of tetrahedron. As shown in Fig. 13a, the smooth distribution of screen element luminance variations does not create false contours.

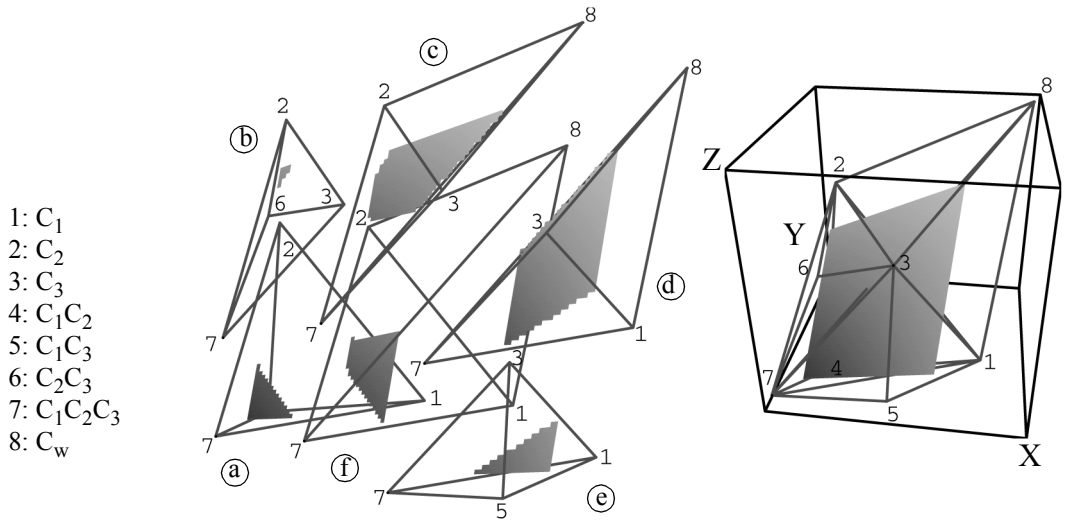

Figure 12. Tetrahedrization with all the tetrahedra with the darkest color as a common vertex.

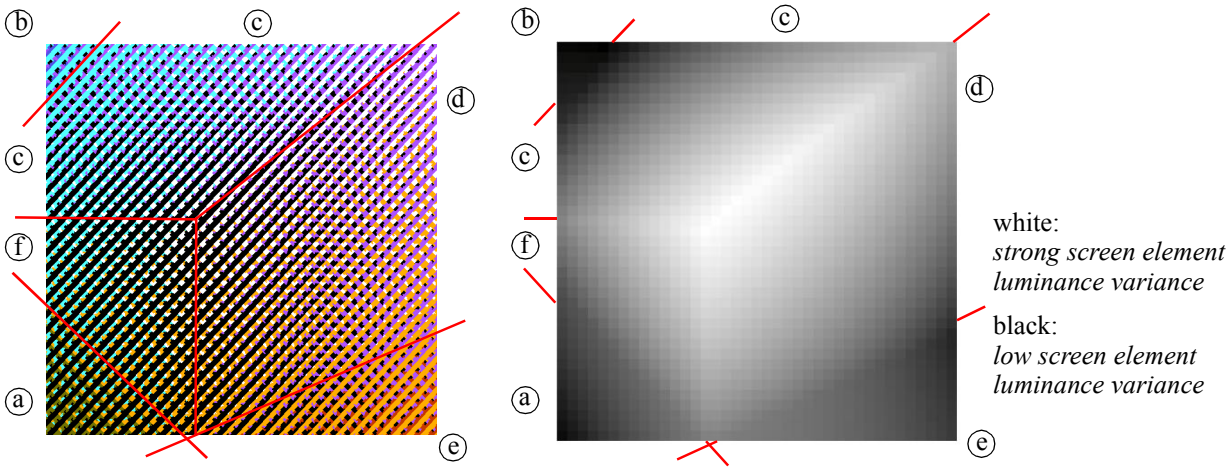

(a) Wedge (b) Screen element luminance variance

Figure 13. Tetrahedrization with all the tetrahedra with the darkest color as a common vertex.

6. IMAGE REPRODUCTION

When rendering an image with multi-color dithering, different tetrahedrizations of the color gamut yield different halftone images having the same global color appearance but different textures. Figures 14 and 15 show an example of a single image produced with two different tetrahedrizations.

Figure 14 is produced with a Delaunay tetrahedrization and Figure 15 with a tetrahedrization maximizing the number of tetrahedra around the dark-white axis.

When viewed from a certain distance, Fig. 14a and Fig. 15a have a similar appearance. However artifacts appear in figure 14a between the highlight part of the face and the dark part of the face, and between the chest and the neck. These artifacts produce interesting artistic effects, but are only welcome in special designs. In contrast, in the image of Fig. 15a no artifacts are visible. The luminance variance (Fig. 14b) shows that Delaunay tetrahedrization creates two areas with two strongly different levels of luminance variance. In contrast, the luminance variance in Fig. 15b follows the luminance information of the original image and therefore does not generate false contours.

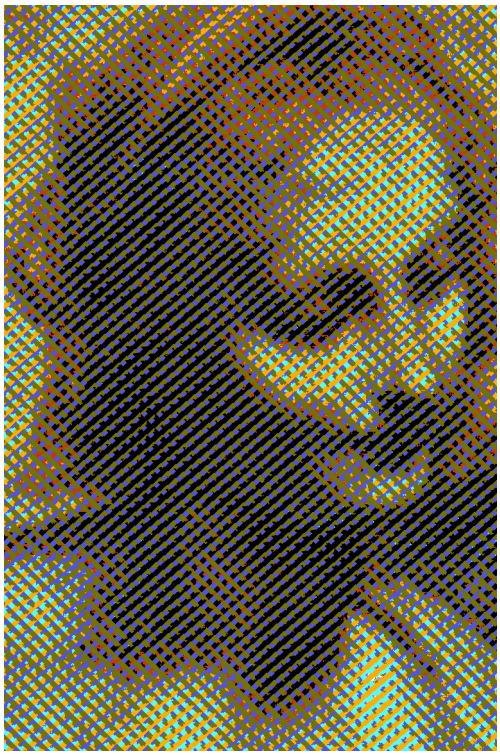

(a) Color image reproduction

(b) Screen element luminance variance

Figure 14. Color image reproduction with Delaunay tetrahedrization.

white:
strong screen element luminance variance

black:
low screen element luminance variance

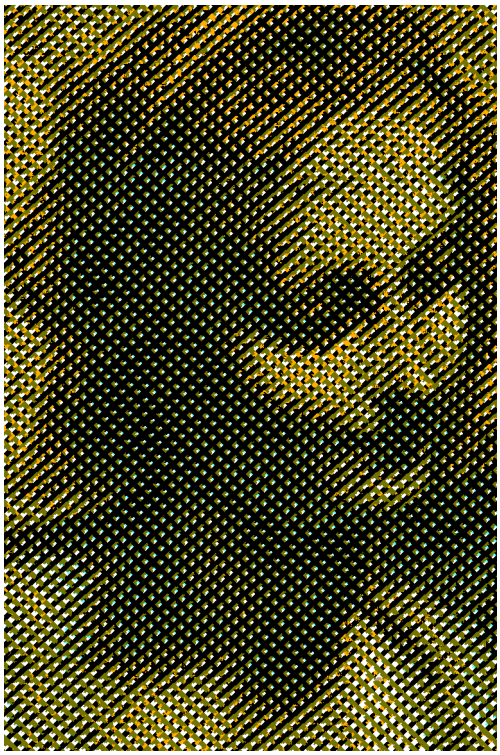

(a) Color image reproduction

(b) Screen element luminance variance

Figure 15. Color image reproduction with a tetrahedrization along the dark-white axis.

7. CONCLUSIONS AND PERSPECTIVES

In this contribution, we study various tetrahedrizations of the color space for printing with a given set of custom inks. We analyze the resulting dithered images, especially in the case of large visible screen tiles. We explain the artifacts produced by certain tetrahedrizations. Artifacts are mostly due to strong spatial variations in screen element luminance variance at boundaries between neighboring tetrahedra. We propose a set of criteria producing tetrahedra minimizing the appearance of false contours due to visible screen element frequency breaks. One criterion maximizes the mean luminance differences of tetrahedron's vertices; the second criterion maximizes the variance in luminance differences of tetrahedron's vertices; a third criterion selects a tetrahedrization with tetrahedra incorporating two vertices with the greatest luminance difference; and a fourth criterion selects a tetrahedrization with a maximum number of tetrahedra incorporating the darkest color.

These criteria don't ensure, for all images, artifact-free dithering. They however reduce the probability of false contours. Sometimes breaks in visible screen element frequency yield interesting artistic effects, which could be of interest for artwork in the fields of publicity or banknote design. We intend to generalize the present study for printing with more than 3 primary inks.

8. ACKNOWLEDGMENTS

We would like to thank Nicolas Rudaz, Isaac Amidror, Patrick Emmel and Edouard Forler for helpful discussions. We also would like to thank Victor Ostromoukhov for having started the research on color separation for custom inks, in collaboration with Orell-Füssli Security Printing Ltd. This project is partially funded by the Swiss CTI (grant 3776.1) and by the Swiss National Science Foundation (grant 21-54127.98).

9. REFERENCES

[1] H. Boll, *A Color to Colorant Transformation for a Seven Ink Process,* in Device Independent Color Imaging, Proc. SPIE, Vol. 2170, pages 108-118, 1994.

[2] E. J. Stollnitz, V. Ostromoukhov, D. H. Salesin, *Reproducing Color Images Using Custom Inks*, Proc. of SIGGRAPH 98, ACM Computer Graphics, Annual Conference Series, pages 267-274, 1998.

[3] V. Ostromoukhov, *Chromaticity Gamut Enhancement by Heptatone Multi-Color Printing*, in Device-Independent Color Imaging and Color Imaging Systems Integration, Proc. SPIE, Vol. 1909, pages 139-151, 1993.

[4] G. Marcu, S. Abe, *Color separation for printing with non-standard inks*, Proc. ICIP-94, IEEE Press, Vol. 3, pages 1002-1005, 1994.

[5] V. Ostromoukhov, Roger D. Hersch, *Multi-Color and Artistic Dithering*, Proc. of SIGGRAPH 99, ACM Computer Graphics, Annual Conference Series, pages 425-432, 1999.

[6] G. M. Nielson, H. Hagen, H. Müller, *Scientific Visualization*, IEEE Computer Society, Chapter 20, 1997.

[7] N. Kathoh, M. Ito, S. Ohno, *Three-dimensional gamut mapping using various color difference formulae and color space*, Journal of Electronic Imaging, Vol. 8(4), pages 365-379, October 1999.

[8] K. Douglas Gennetten, *RGB to CMYK conversion using 3D barycentric interpolation*, Device-Independent Color Imaging and Imaging Systems Integration, Proc. of SPIE, vol. 1909, pages 116-126, February 1993.

[9] Y. Zhang, R.E. Webber, *Space Diffusion: An Improved Parallel Halftoning Technique Using Space-Filling Curves*, Proc. of SIGGRAPH 93, ACM Computer Graphics, Annual Conference Series, pages 305-312, 1993.

[10] Luiz Velho and Jonas de Miranda Gomes, *Space-Filling Curve Dither with Adaptive Clustering*, Proc. of SIGGRAPH 91, ACM Computer Graphics, Vol. 25, No. 4, pages 81-90, July 1991.

Appendix. Dithered color images.

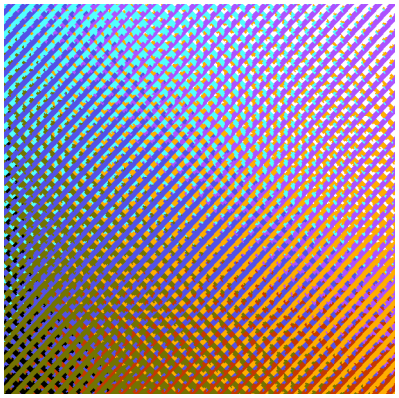

Fig. 5a Delaunay tetrahedrization.

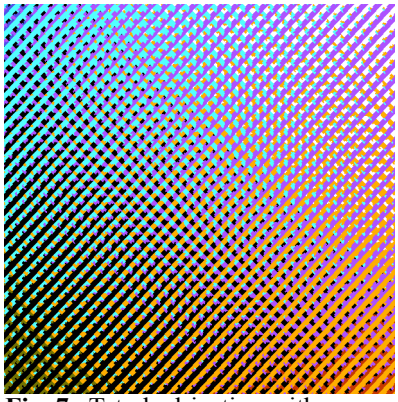

Fig. 7a Tetrahedrization with five tetrahedra.

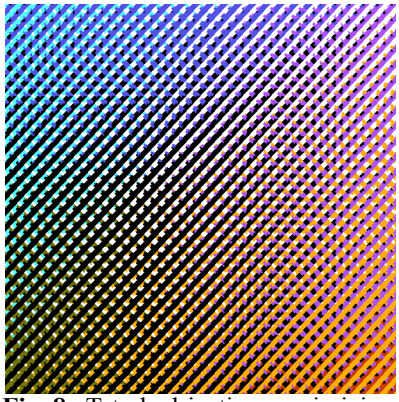

Fig. 8a Tetrahedrization maximizing the mean luminance differences.

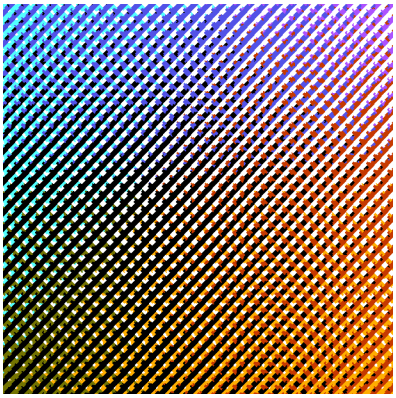

Fig. 9a Tetrahedrization maximizing the variance in luminance differences.

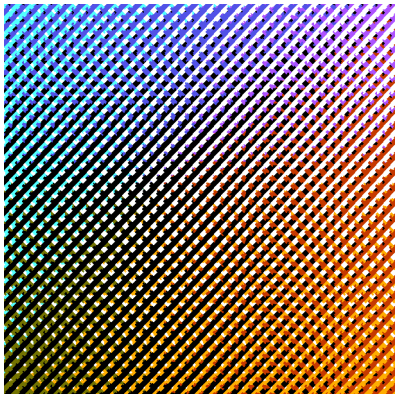

Fig. 11a Tetrahedrization around the dark-white axis.

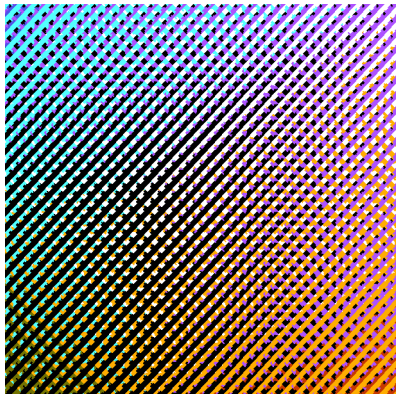

Fig. 13a Tetrahedrization with all the tetrahedra with the darkest color.

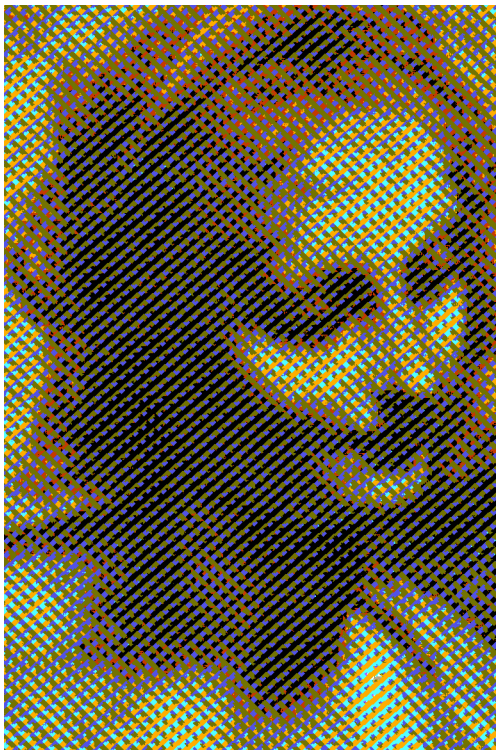

Fig. 14a Delaunay tetrahedrization.

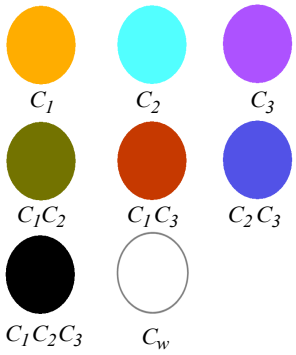

Fig. 1
Set of basic colors.

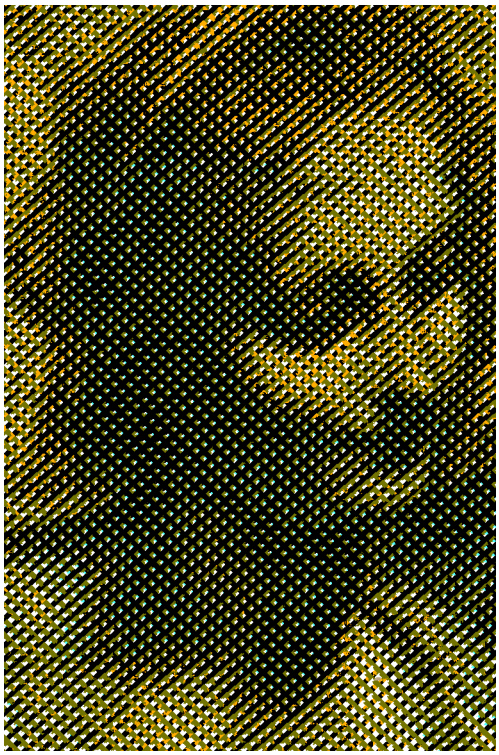

Fig. 15a Tetrahedrization along the dark-white axis.